Vol. 2, No. 2, October 2026, Page 122-135 E-ISSN 3123-4674

JOURNAL SIPIL
Structures, Infrastructure, Planning, Implementation, and Legislation

Utilization of Nickel Slag as Coarse Aggregate Replacement in High-Strength Concrete

Rahayu Amanda[1]*, & Muhammad Yose[2]
[1]*Universitas Bung Hatta, Indonesia, [2]Universitas Putra Indonesia "YPTK" Padang, Indonesia
*Co e-mail: amndaayu@gmail.com[1]

Article Information
Received: September 30, 2026
Revised: October 20, 2026
Online: October 30, 2026

Keywords
Nickel Slag, Coarse Aggregate, High-Strength Concrete, Compressive Strength

ABSTRACT

Purpose: Nickel smelting in Indonesia generates large quantities of slag, but evidence for its performance as aggregate in high-strength concrete is scattered and partly contradictory. This study reanalyzed two published datasets to test whether nickel slag affects strength and to guide mix proportioning. Methods: A normal-strength series (about 30 MPa; Amir et al., 2022), in which nickel slag replaced crushed-stone coarse aggregate at 0, 10, 25, 50, and 100 %, was reanalyzed with one-way ANOVA, regression, and 95 % confidence intervals. A high-performance series (target 60 MPa; Nelfia et al., 2024), in which nickel slag replaced both fine and coarse aggregate, was analyzed by absolute-volume calculation. Results: In the baseline series, 28-day mean strength ranged only from 30.10 to 30.77 MPa (ANOVA $F = 0.32$, $p = .86$; $R^2 = .007$), and every confidence interval for the difference from the control (−2.17 to +1.12 MPa) included zero, so no strength penalty was demonstrated up to 100 % replacement. In the high-performance series, the highest reported strength (69.43 MPa, 11.56 % above the reference) occurred at 40 % replacement, where slag replaced 589 kg/m^3 of natural aggregate. Mass-for-mass replacement left a computed volume deficit of up to 75 L/m^3 because nickel slag is denser (specific gravity 2.95 versus 2.60–2.62) and less absorptive; volume-based replacement would raise concrete density by 4.1 % at 40 % replacement. Conclusion: Because the data are published rather than new, the results are intended to guide mix proportioning and to define a validation program for high-strength concrete.

Keywords: *Nickel Slag, Coarse Aggregate, High-Strength Concrete, Compressive Strength*

DOI: http://doi.org/10.69855/sipil.v2i2.902
Available online at website: https://gpijournal.com/index.php/sipil
PUBLISHED BY : GPress Indonesia

This work is licensed under a Creative Commons Attribution 4.0 International license

INTRODUCTION

Indonesia is the world's largest producer of nickel, and the expansion of domestic smelting following the 2020 ban on raw ore exports has increased the generation of nickel slag, a by-product that is produced in much larger quantity than the metal itself (Nelfia et al., 2024). Slag disposal occupies land and creates environmental liabilities, while the construction sector continues to consume large volumes of natural sand and crushed stone. Using slag as aggregate in concrete addresses both problems, and for high-strength concrete (HSC), where the aggregate occupies about two-thirds of the volume and controls stiffness and the strength of the interfacial transition zone (Mehta & Monteiro, 2014; Neville, 2011), the choice of coarse aggregate is particularly important (Aïtcin & Mehta, 1990; Beshr et al., 2003).

A substantial literature now addresses slag from nickel and ferronickel production as a fine aggregate. Ferronickel slag sand has been reported to increase density, compressive strength, pulse velocity, and stiffness of concrete while reducing Poisson's ratio (Ernawan et al., 2023); blends of quarry dust and ferronickel slag as full sand replacement gave concrete about 16 % stronger than the control (Nuruzzaman et al., 2024); and nickel slag sand has been studied in self-compacting concrete (Nuruzzaman et al., 2020, 2022; Fitriyanti et al., 2025), in marine environments with fly ash (Ahmad et al., 2022), and with regard to reinforcement corrosion (Irmawaty et al., 2023). Ferronickel slag aggregate has also been used in seawater concrete (Sandra et al., 2025), and iron slag together with stone ash has been used to replace aggregate in self-compacting concrete (Adiwijaya et al., 2026). By comparison, the use of nickel slag as coarse aggregate has been examined far less, and the few available studies point in different directions. A study on normal-strength concrete found no benefit and advised against use in structural concrete of 20 MPa and above (Amir et al., 2022), whereas a high-performance concrete series using slag for both fine and coarse aggregate found the highest strength at an intermediate replacement level (Nelfia et al., 2024). Studies of steel slag and nickel slag as coarse aggregate in high-quality concrete have also been reported in Indonesia (Suwindu et al., 2020), and other industrial slags used as coarse aggregate have shown a similar peak at moderate replacement (Soundararajan et al., 2023). Steel slag and electric arc furnace (EAF) slag have likewise been examined as coarse aggregate, and in some cases gave higher strength and stiffness than conventional concrete (Coppola et al., 2016; Rojas et al., 2023), while the properties of steel slag concrete have also been compared with those of crushed limestone aggregate concrete (Maslehuddin et al., 2003).

These reports differ in strength class, binder system, replacement ratio, and specimen size, and most contain few specimens per condition. As a result, it is difficult for a practitioner to judge whether the differences reported between mixes reflect a real material effect or ordinary test scatter, and how the physical properties of the slag should influence mix proportioning. A statistical re-examination of the available specimen-level data, together with a volumetric analysis of published mix proportions, can help to resolve these questions without new tests.

The objectives of this study are therefore (i) to test statistically whether replacing crushed stone with nickel slag, from 0 to 100 %, changes the compressive strength and early-age strength development of concrete; (ii) to compare the physical properties of nickel slag coarse aggregate reported by two independent sources; (iii) to quantify, by absolute-volume analysis of published high-performance mixes, how replacement by mass changes the volume balance, density, absorbed water, and consumption of natural aggregate; and (iv) to place these findings in the context of the wider slag-aggregate literature and to identify what an experimental validation should measure. The contribution is an integrated and transparent analysis of published evidence; it is not a new laboratory investigation, and this is stated so that the results are interpreted accordingly.

This work is licensed under a Creative Commons Attribution 4.0 International license

METHODS

1. Study design

A quantitative secondary analysis was carried out on two experimental studies from Indonesian laboratories that used nickel slag from Southeast Sulawesi as aggregate. Dataset A is the specimen-level strength data of Amir et al. (2022), who replaced crushed stone coarse aggregate by nickel slag at 0, 10, 25, 50, and 100 % and tested three cylinders per replacement level at 1, 3, 7, 14, and 28 days. Dataset B is the material properties and mix proportions of Nelfia et al. (2024), who produced high-performance concrete with a water-to-binder ratio of 0.317, 20 % ground granulated blast-furnace slag (GGBFS) as cement replacement, and nickel slag replacing both the fine and the coarse aggregate at 0, 20, 40, 60, 80, and 100 % (mixes Ref, Mix 1 to Mix 5), designed according to ACI 211.4R (ACI Committee 211, 2008) for a target strength of 60 MPa. All values were transcribed from the published tables and text; numerical values that were internally inconsistent in a source (for example, fineness modulus and abrasion values in Amir et al., 2022) were not used. The strength values that Nelfia et al. (2024) present only graphically were not extracted; only numbers stated in their text and tables were used.

2. Physical properties of aggregates

The specific gravity in saturated-surface-dry condition (SSD) and water absorption of natural and slag aggregates reported in the two studies were tabulated (Table 1). Specific gravity and absorption of coarse aggregate are conventionally measured by standard test methods such as ASTM C127 (ASTM International, 2015). The comparison serves as an independent check on the consistency of the slag properties between the two sources, which were tested in different laboratories.

Table 1. Physical properties of natural and nickel slag aggregates reported in the two source studies

Property	Crushed stone (Amir et al.)	Nickel slag (Amir et al.)	Natural coarse (Nelfia et al.)	Nickel slag coarse (Nelfia et al.)
Specific gravity, SSD (coarse)	2.62	2.95	2.60	2.95
Water absorption, % (coarse)	2.84	0.91	1.68	0.86
Specific gravity, SSD (fine)	2.51 (river sand)	–	2.51 (natural sand)	3.06 (nickel slag sand)
Water absorption, % (fine)	1.78 (river sand)	–	2.78 (natural sand)	0.91 (nickel slag sand)

3. Statistical analysis of compressive strength (Dataset A)

For each replacement level and age the mean, sample standard deviation (SD), and coefficient of variation (CV) were computed from the three specimen strengths. Because n = 3 per group, the sample SD is itself uncertain, and the results are interpreted with confidence intervals rather than significance alone. Differences among replacement levels at each age were tested by one-way analysis of variance (ANOVA), and Tukey's honestly significant difference test (Tukey, 1949) was applied to the 28-day data. Homogeneity of variance was checked with Levene's test (Levene, 1960). The 28-day strengths of all 15 specimens were regressed on the replacement percentage. The 95 % confidence interval of the

This work is licensed under a Creative Commons Attribution 4.0 International license

difference between each replacement level and the control was calculated with the pooled within-group variance:

$$\Delta \pm t_{0.975,10} \cdot s_p \sqrt{(2/n)} \quad (1)$$

where Δ is the difference of the group means, s_p is the pooled SD (0.83 MPa at 28 days, 10 degrees of freedom), and n = 3. Analyses were run in Python with the SciPy library (Virtanen et al., 2020).

4. Volumetric analysis of mix proportions (Dataset B)

The reported mix proportions (kg/m^3) were converted to absolute volumes using the specific gravity of each constituent (cement 3.13, GGBFS 2.83, superplasticizer 1.05, water 1.00, and aggregates as in Table 1):

$$V_i = m_i / \rho_i, \quad V_{air} = 1000 - \Sigma V_i \quad (2)$$

where m_i is the mass of constituent i per m^3 and ρ_i is its specific gravity (kg/L). The term V_{air} is the implied void volume; for a well-proportioned mix it should be small and positive. The water that the aggregates can absorb was estimated assuming the reported masses to be oven-dry:

$$W_{abs} = \Sigma\, m_a \cdot A_a / 100 \quad (3)$$

where A_a is the water absorption (%) of aggregate fraction a. To show the effect of replacing aggregate by volume instead of by mass, the mass of slag that occupies the same volume as the natural aggregate it replaces was computed:

$$m_{NS} = r \cdot m_{NA} \cdot (\rho_{NS} / \rho_{NA}) \quad (4)$$

where r is the replacement fraction, m_{NA} is the mass of natural aggregate in the reference mix, and ρ_{NS} and ρ_{NA} are the specific gravities of slag and natural aggregate. The density of the volume-based mixes is the sum of the constituent masses. Finally, the elastic modulus was estimated from the compressive strength with the empirical expression for high-strength concrete of ACI Committee 363 (2010), valid for 21 to 83 MPa:

$$E_c = 3320 \sqrt{f'_c} + 6895 \quad \text{(MPa)} \quad (5)$$

This expression was calibrated on natural aggregates, so it gives only an indicative value for slag concrete, because the stiffness of high-strength concrete depends on the type of coarse aggregate (Aïtcin & Mehta, 1990; Mehta & Monteiro, 2014). The reference-mix strength was derived from the reported values as $f'_{c,Ref}$ = 69.43 / 1.1156 = 62.2 MPa.

RESULTS

1. Physical properties of nickel slag aggregate

The two independent sources agree closely on the properties of nickel slag coarse aggregate (Table 1, Figure 1). The specific gravity of the slag was 2.95 in both studies, against 2.62 and 2.60 for the natural coarse aggregates, i.e., the slag is about 13 % denser. The water absorption of the slag was 0.91 and 0.86 %, only about one-third to one-half of the 2.84 and 1.68 % of the natural aggregates. The slag fine aggregate of Nelfia et al. (2024) showed the same tendency (specific gravity 3.06 against 2.51; absorption 0.91 against 2.78 %). The agreement between two laboratories on slag from the same region gives confidence that these two properties are stable enough to be used in mix proportioning.

This work is licensed under a Creative Commons Attribution 4.0 International license
Structures, Infrastructure, Planning, Implementation, and Legislation (SIPIL)
Vol. 2, No. 2, October 2026

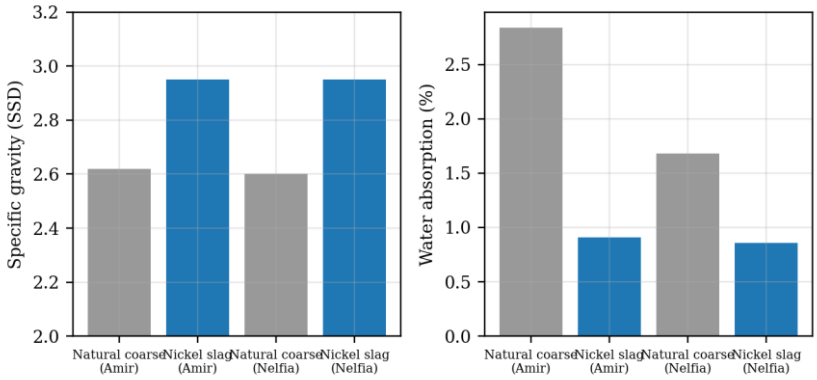


Figure 1. Specific gravity (SSD) and water absorption of natural and nickel slag coarse aggregates reported by the two source studies

2. Strength development with coarse nickel slag

Figure 2 shows the mean strength with one SD at each age. At 28 days the mean strengths were 30.77 MPa (control), 30.26, 30.10, 30.13, and 30.38 MPa for 10, 25, 50, and 100 % slag (Table 2). The largest difference from the control was −0.66 MPa (−2.2 %) at 25 % replacement. The scatter within groups decreased with increasing slag content at 28 days (CV from 4.6 % in the control to 0.6 % at 100 % slag), although Levene's test did not show that the variances differed significantly (p = .77).

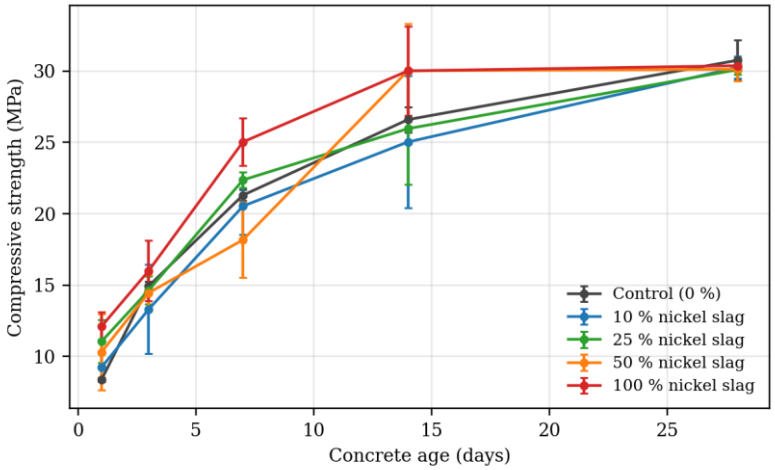


Figure 2. Compressive strength development of concrete with 0 to 100 % of the coarse aggregate replaced by nickel slag (mean ± 1 SD, n = 3; data from Amir et al., 2022)

Strength development at early ages appeared faster with high slag contents. At 7 days the 100 % slag concrete reached 25.0 MPa, or 82.4 % of its 28-day strength, against 21.3 MPa (69.2 %) for the control; at 14 days the values were 30.0 MPa (98.8 %) and 26.6 MPa (86.5 %), respectively. In contrast, the 50 % replacement gave the lowest 7-day mean (18.2 MPa) but a high value at 14 days (30.0 MPa), so the early-age pattern is not monotonic in replacement level.

This work is licensed under a Creative Commons Attribution 4.0 International license

Table 2. Compressive strength at 28 days and difference from the control (computed from specimen data of Amir et al., 2022)

Replacement (%)	n	Mean (MPa)	SD (MPa)	CV (%)	Δ vs. control (MPa)	95 % CI of Δ (MPa)	Δ (%)
0	3	30.77	1.42	4.6	–	–	–
10	3	30.26	0.76	2.5	−0.51	−2.01 to 1.00	−1.6
25	3	30.10	0.36	1.2	−0.66	−2.17 to 0.84	−2.2
50	3	30.13	0.83	2.8	−0.64	−2.14 to 0.87	−2.1
100	3	30.38	0.18	0.6	−0.39	−1.89 to 1.12	−1.3

3. Statistical significance

The one-way ANOVA of the 28-day strengths gave $F(4,10) = 0.32$ and $p = .86$ (Table 3), and Tukey's test found no pair of groups that differed (smallest adjusted $p = .86$). The linear regression of the 15 specimen strengths on replacement level had a slope of −0.002 MPa per percentage point ($R^2 = .007$, $p = .76$; Figure 3), that is, a predicted change of −0.17 MPa over the full range of 0 to 100 %. The 95 % confidence interval of the difference from the control was between −2.17 and +1.12 MPa for all four replacement levels (−7.1 % to +3.6 % of the control mean), so all include zero. The only age at which the ANOVA was significant was 7 days ($p = .007$), which reflects the contrast between the low 50 % group and the high 100 % group rather than a trend.

Table 3. One-way ANOVA of compressive strength among replacement levels at each age

Age (days)	Control mean (MPa)	100 % slag mean (MPa)	F(4,10)	p-value	Interpretation
1	8.4	12.1	2.85	.082	Not significant
3	14.9	16.0	0.84	.529	Not significant
7	21.3	25.0	6.67	.007	Significant
14	26.6	30.0	1.41	.298	Not significant
28	30.8	30.4	0.32	.861	Not significant

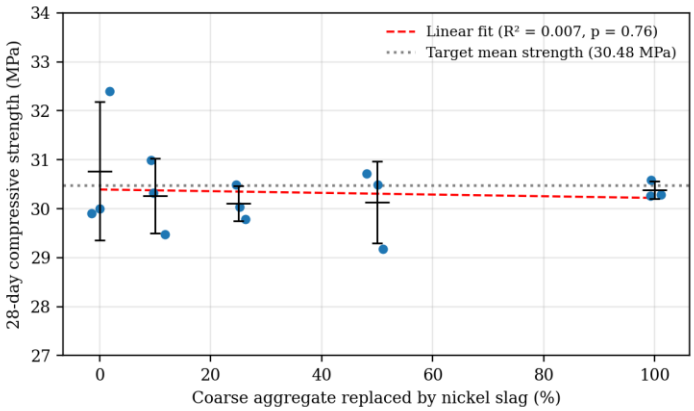


Figure 3. Individual 28-day strengths (points), group means ± 1 SD (bars), linear regression (dashed), and the target mean strength of 30.48 MPa (dotted); data from Amir et al. (2022)

This work is licensed under a Creative Commons Attribution 4.0 International license
Structures, Infrastructure, Planning, Implementation, and Legislation (SIPIL)
Vol. 2, No. 2, October 2026

The design target mean strength in the source study was 30.48 MPa. The control mean (30.77 MPa) exceeded it by 0.29 MPa, whereas the slag concretes fell below it by 0.10 to 0.38 MPa. However, only 1 of the 3 control specimens and 1 of the 3 specimens with 100 % slag reached the target, and 2 of the 3 specimens with 50 % slag did, so the pass–fail outcome relative to the target lies within the specimen-to-specimen scatter (pooled SD 0.83 MPa).

4. Volume balance and density of the high-performance mixes

Table 4 shows the results of the absolute-volume analysis of the six high-performance mixes of Nelfia et al. (2024). In the reported proportions the total mass of every mix is the same (2,322 kg/m^3) because slag replaced natural aggregate by mass, but slag is denser than natural aggregate, so the computed solid and water volume declined steadily from 986 L/m^3 in the reference mix to 911 L/m^3 in Mix 5, a reduction of 75 L/m^3 (7.6 %). The implied void volume therefore increased from 14.0 L/m^3 (1.4 %) to 88.9 L/m^3 (8.9 %); at 40 % replacement (Mix 2) it was 41.3 L/m^3 (4.1 %). The reported quantities cannot be checked against the actual batching, so this is a property of the reported proportions and not measured void content. The volume-based alternative of Eq. (4) would increase the concrete density from 2,322 kg/m^3 to 2,417 kg/m^3 (+4.1 %) at 40 % and to 2,559 kg/m^3 (+10.2 %) at 100 % replacement.

Table 4. Absolute-volume analysis of the mix proportions of Nelfia et al. (2024) (NS = nickel slag; "Implied voids" = 1000 − Σ volumes; "Vol.-based density" from Eq. (4))

Mix	Repl. (%)	Coarse NS (kg/m^3)	Total NS (kg/m^3)	Natural agg. (kg/m^3)	Σ volume (L/m^3)	Implied voids (L/m^3)	Absorbed water (kg/m^3)	Vol.-based density (kg/m^3)
Ref	0	0	0	1,474	986	14	29.8	2,322
Mix 1	20	203	295	1,179	975	25	26.4	2,369
Mix 2	40	405	589	884	959	41	23.1	2,417
Mix 3	60	608	884	589	943	57	19.7	2,464
Mix 4	80	810	1,179	295	927	73	16.3	2,512
Mix 5	100	1,013	1,474	0	911	89	12.9	2,559

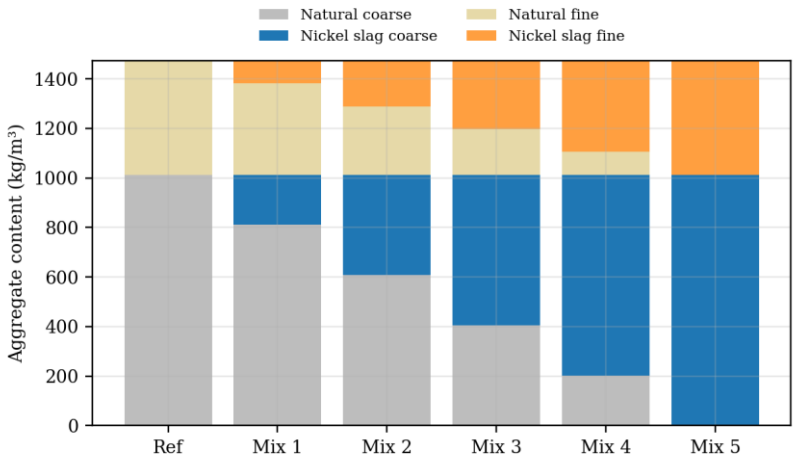


Figure 4. Aggregate composition per m^3 of the reference mix and mixes with 20 to 100 % nickel slag (mass-based replacement; data from Nelfia et al., 2024)

This work is licensed under a Creative Commons Attribution 4.0 International license

The lower absorption of the slag also changes the water balance. If the reported masses are taken as oven-dry, the aggregates of the reference mix can absorb 29.8 kg/m^3 of water (14.7 % of the mixing water of 202.6 kg/m^3), and this falls to 23.1 kg/m^3 at 40 % and 12.9 kg/m^3 at 100 % slag (Table 4). In a mix with a water-to-binder ratio as low as 0.317, this 6.7 to 16.9 kg/m^3 difference in absorbed water is equivalent to 3 to 8 % of the mixing water, so the effective water-to-binder ratio of a slag mix will differ from that of the reference unless the aggregate moisture condition is controlled.

5. Reported performance of the high-performance mixes

Nelfia et al. (2024) reported that the best compressive strength (69.43 MPa at 28 days) occurred at 40 % replacement (Mix 2), 11.56 % above the reference, which corresponds to a reference strength of 62.2 MPa; that the gas permeability coefficient of Mix 2 was 31.06 % lower than that of the reference (6.11×10^{-8}); and that its porosity was 6.52 %, 11.57 % below the reference. They also reported that the other slag mixes were below the reference strength (a decrease of 20.28 % is quoted), and that the highest tensile strength (5.27 MPa) was obtained in Mix 3. Table 5 summarises these figures together with the elastic moduli estimated with Eq. (5), which are 33.1 GPa for the reference and 34.6 GPa for Mix 2, an increase of 4.4 % that follows from the higher strength alone and is not a measurement.

Table 5. Performance of the reference mix and the best mix (Mix 2) reported by Nelfia et al. (2024), with derived values

Property	Reference (Ref)	Mix 2 (40 % nickel slag)	Change	Basis
28-day compressive strength (MPa)	62.2	69.4	+11.56 %	Reported (Ref derived)
Gas permeability coefficient ($\times 10^{-8}$)	6.11	4.21	−31.06 %	Reported (Mix 2 derived)
Porosity (%)	7.37	6.52	−11.57 %	Reported (Ref derived)
Elastic modulus, E_c (GPa)	33.1	34.6	+4.4 %	Computed, Eq. (5)

6. Resource utilization

In Mix 2 the total slag aggregate was 589 kg/m^3 (405 kg/m^3 coarse and 184 kg/m^3 fine), about 25 % of the concrete mass, and it replaced an equal mass of natural aggregate (40 % of 1,474 kg/m^3). The coarse slag occupied 137 L/m^3, or 37 % of the coarse aggregate volume. In addition, 127.8 kg/m^3 of cement (20 %) was replaced by GGBFS in all slag mixes. At 100 % replacement, all 1,474 kg/m^3 of natural aggregate is displaced (Figure 5).

This work is licensed under a Creative Commons Attribution 4.0 International license
Structures, Infrastructure, Planning, Implementation, and Legislation (SIPIL)
Vol. 2, No. 2, October 2026

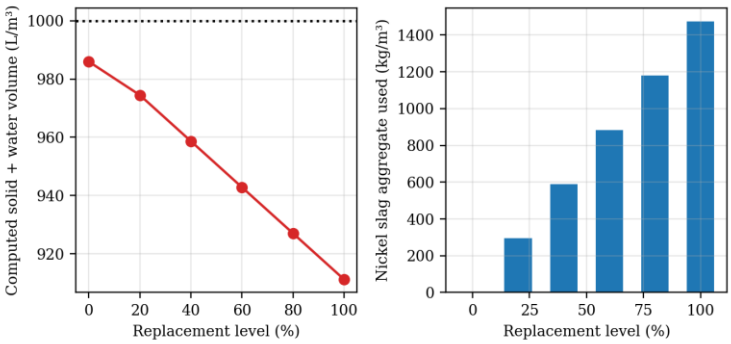


Figure 5. (Left) Computed solid and water volume per m³ for mass-based replacement, with the 1000 L target (dotted); (Right) mass of nickel slag aggregate used per m³ (data from Nelfia et al., 2024)

DISCUSSION

1. Coarse nickel slag does not appear to reduce strength

The re-analysis does not support the impression, given by the conclusion of the normal-strength study, that coarse nickel slag lowers concrete strength. The 28-day strengths were statistically indistinguishable across 0 to 100 % replacement, the regression slope was practically zero, and the confidence intervals of the differences (−2.2 to +1.1 MPa) are narrow enough to exclude a large loss but wide enough to include a small one. The source authors concluded that nickel slag is not recommended for structural concrete of 20 MPa and above because the slag mixes did not reach the design target mean strength (Amir et al., 2022). The present analysis shows that this shortfall of 0.1 to 0.4 MPa is far smaller than the scatter among specimens and that the control itself exceeded the target only by 0.29 MPa; the conclusion is therefore better read as a failure to demonstrate an improvement than as a demonstration of a deficiency. With only three specimens per group, effects smaller than about 1.5 MPa cannot be resolved, and this is the main statistical limitation.

The behavior is consistent with the properties in Table 1. Slag with a specific gravity of 2.95 and an absorption below 1 % is a dense aggregate with a low porosity, and these are properties that normally favor strength and durability of the interfacial transition zone and aggregate (Mehta & Monteiro, 2014; Neville, 2011). The faster early strength development of the 100 % slag group may be related to the low absorption and the glassy, angular surface of the particles, but the data are too scattered at 7 and 14 days (SD up to 4.6 MPa) to confirm this, and the ANOVA at 14 days was not significant (p = .30).

2. Why the high-performance series peaked at an intermediate replacement

The high-performance series of Nelfia et al. (2024) found the highest strength at 40 % replacement, and other industrial slag aggregates used for coarse aggregate in M60 high-performance concrete have also peaked at about 30 % (Soundararajan et al., 2023; Table 6). Two observations from the volumetric analysis help to interpret such a peak. First, for mass-based replacement the volume of solids decreases as slag content increases, and the implied void volume increases from 14 L/m³ to 89 L/m³; a higher void content would increasingly offset any benefit of the denser aggregate and could explain the decline at high replacement levels. Second, the reduction of absorbed water with slag content changes the effective water-to-binder ratio. At 40 % replacement, 6.7 kg/m³ less water would be absorbed than in the reference mix, which is a modest change, whereas at 100 % the change is 16.9 kg/m³. Both effects act in the same direction and grow with the replacement level, whereas the benefit of a denser, less porous aggregate saturates. This explanation is a hypothesis based on the reported

This work is licensed under a Creative Commons Attribution 4.0 International license

proportions; the data do not allow the roles of the void volume, the effective water, and the aggregate to be separated, and it should be tested by measuring the fresh density and air content of each mix.

Table 6. Summary of reported results for slag used as aggregate in concrete

Study	Slag material and role	Replacement / strength class	Reported outcome
Amir et al. (2022)	Nickel slag, coarse aggregate	0–100 % / ≈30 MPa	No strength gain; authors do not recommend for ≥20 MPa concrete
Nelfia et al. (2024)	Nickel slag, fine + coarse aggregate; 20 % GGBFS	0–100 % / ≈60 MPa target	Peak 69.43 MPa at 40 % (+11.56 %); lower porosity and permeability
Soundararajan et al. (2023)	Ferro slag aggregate, coarse aggregate	0–40 % / M60 HPC	Peak 71.20 MPa at 30 %, ≈30 % above conventional concrete; decline at 40 %
Ernawan et al. (2023)	Ferronickel slag, fine aggregate	0, 50, 100 %	Higher density, strength, pulse velocity, stiffness; lower Poisson's ratio
Nuruzzaman et al. (2024)	Ferronickel slag with quarry dust, fine aggregate	Full sand replacement	Best blend (QD25–FNS75) 16 % stronger than control
Fitriyanti et al. (2025)	Nickel slag, fine aggregate in SCC	Optimum level	Strength above control while meeting SCC requirements

3. Mass-based and volume-based replacement

The finding that mass-for-mass replacement leaves a volume deficit of 75 L/m^3 at full replacement has practical importance, because the specific gravity of nickel slag is 13 % higher than that of the natural aggregates it replaces. Mix design procedures such as ACI 211.4R (ACI Committee 211, 2008; Aïtcin, 1998) proportion the aggregates by absolute volume, and a slag aggregate should therefore be introduced by volume, with the bulk density, specific gravity, and absorption of the slag measured for the specific source. On this basis, the concrete would be 4.1 % denser at 40 % replacement and 10.2 % denser at 100 % replacement, an important point for the self-weight of structural members and the design of formwork and foundations, which is an effect that does not appear when the mass of the aggregate is held constant. It also means that the comparison of strength between mixes in the source study is a comparison of mixes that differ in paste-to-aggregate volume ratio and voids, in addition to the slag content, and that the strength of the slag mixes may be underestimated if the deficit was real.

4. Sources of variability that a validation must control

Slag from different smelters and from different ore types differs in chemical composition, in vesicularity, and in grain shape, which is an issue emphasized by Nelfia et al. (2024), who noted that lateritic ores give slag with a high iron oxide content and a different mineralogy from slag of sulfide ores. The slag used in the two studies was of Southeast Sulawesi origin, which may explain their agreement on physical properties, but it is not evidence that slag from other sources will behave in the same way.

This work is licensed under a Creative Commons Attribution 4.0 International license

The leaching of nickel is another consideration: the toxicity characteristic leaching test reported by Nelfia et al. (2024) gave 7.47 mg/L for nickel from the slag, above the 5 mg/L limit they cite for hazardous waste characterization, and this should be assessed for concrete in contact with groundwater. Leachate from steel slag aggregate concrete has likewise been assessed against legal limits (Diotti et al., 2021). Finally, the presence of GGBFS in the high-performance series, and the simultaneous replacement of fine and coarse aggregate, mean that the effect of the coarse fraction alone cannot be isolated from the published data.

5. Recommendations for experimental validation

A validation program should replace only the coarse aggregate by volume, at about 0, 25, 40, 50, and 100 %; use a single binder system of a high-strength type (water-to-binder ratio of about 0.30 to 0.35, with superplasticizer); test at least six cylinders per mix (e.g., following ASTM C39/C39M; ASTM International, 2021), since three cannot resolve a difference below about 1.5 MPa; record fresh density, air content, and slump; control the aggregate moisture condition and report the effective water-to-binder ratio; and measure the elastic modulus (e.g., by ASTM C469/C469M; ASTM International, 2014), splitting tensile strength, and permeability in addition to compressive strength, since the stiffness of HSC depends strongly on the coarse aggregate. Nickel leaching of the concrete should also be checked.

6. Limitations

The main limitation is that the study is a secondary analysis and contains no new laboratory measurements. The specimen-level statistics rest on three specimens per condition from one laboratory, and the strength values of the high-performance series are available only as reported summary figures. The two datasets differ in strength class, binder, and the fractions replaced, and are analyzed side by side and not pooled. The volumetric calculations assume that the reported masses and SSD specific gravities are exact and that the aggregates were batched oven-dry; if the actual batching differed, the void and water estimates would change. The modulus estimate is empirical and was not calibrated for slag aggregate. Finally, durability, shrinkage, creep, and long-term behavior were not addressed.

CONCLUSIONS

A statistical and volumetric re-analysis of two published datasets on nickel slag aggregate in concrete leads to the following conclusions. First, nickel slag coarse aggregate from Southeast Sulawesi is denser and less absorptive than natural coarse aggregate: two independent studies gave a specific gravity of 2.95 (against 2.60–2.62) and absorption of 0.86–0.91 % (against 1.68–2.84 %). Second, in normal-strength concrete (≈30 MPa), replacing crushed stone by 10 to 100 % of nickel slag did not change the 28-day strength in a statistically detectable way (means 30.10–30.77 MPa; ANOVA $p = .86$; $R^2 = .007$), and all confidence intervals of the differences (−2.17 to +1.12 MPa) included zero. Third, the reported shortfall of the slag mixes relative to the design target (0.1–0.4 MPa) is smaller than the scatter among specimens, so the recommendation against use at 20 MPa and above is not supported by the strength data alone. Fourth, in the high-performance series (target 60 MPa, 20 % GGBFS) the highest reported strength was 69.43 MPa (+11.56 %) at 40 % replacement of both fine and coarse aggregate, with 31 % lower permeability and 11.6 % lower porosity, while other industrial slag aggregates in M60 concrete have peaked at about 30 %. Fifth, mass-based replacement leaves a computed volume deficit growing to 75 L/m^3 (7.6 %) at full replacement; volume-based replacement is recommended and would raise the concrete density by 4.1 % at 40 % replacement, while reducing the water absorbed by the

This work is licensed under a Creative Commons Attribution 4.0 International license

aggregates. Finally, at 40 % replacement, about 589 kg/m^3 of natural aggregate and 128 kg/m^3 of cement are displaced by industrial by-products, and these conclusions should be validated by tests that replace only the coarse aggregate by volume, with adequate replication, before use in design.

REFERENCES

ACI Committee 211. (2008). *Guide for selecting proportions for high-strength concrete with Portland cement and other cementitious materials (ACI 211.4R-08)*. American Concrete Institute.

ACI Committee 363. (2010). *Report on high-strength concrete (ACI 363R-10)*. American Concrete Institute.

Adiwijaya, Irmawaty, R., Datu, I. T., Khairil, Rochman, T., Ridwan, V. F., Suradi, M., Muhammad, A. K., Setiawan, B., & Yatsam, R. (2026). Exploring the potential of iron slag and stone ash as aggregate replacements for the improvement of the compressive strength and durability of self-compacting concrete. *Engineering, Technology & Applied Science Research, 16*(1), 32550–32556. https://doi.org/10.48084/etasr.16741

Ahmad, S. B., Irmawaty, R., Aly, S. H., & Amiruddin, A. (2022). Performance of fly ash concrete with nickel slag fine aggregate in the marine environment. *Civil Engineering Journal, 8*(12), 61–68. https://doi.org/10.28991/CEJ-2022-08-12-010

Aïtcin, P.-C. (1998). *High-performance concrete*. E & FN Spon.

Aïtcin, P. C., & Mehta, P. K. (1990). Effect of coarse aggregate characteristics on mechanical properties of high-strength concrete. *ACI Materials Journal, 87*(2), 103–107. https://doi.org/10.14359/1882

Amir, A. A., Sukman, Mahmud, & Hasrudin. (2022). Use of nickel slag waste as coarse aggregate in concrete. *PENA TEKNIK: Jurnal Ilmiah Ilmu-Ilmu Teknik, 7*(2). https://doi.org/10.51557/pt_jiit.v7i2.1270

ASTM International. (2014). *Standard test method for static modulus of elasticity and Poisson's ratio of concrete in compression (ASTM C469/C469M-14)*. ASTM International.

ASTM International. (2015). *Standard test method for relative density (specific gravity) and absorption of coarse aggregate (ASTM C127-15)*. ASTM International.

ASTM International. (2021). *Standard test method for compressive strength of cylindrical concrete specimens (ASTM C39/C39M-21)*. ASTM International.

Beshr, H., Almusallam, A. A., & Maslehuddin, M. (2003). Effect of coarse aggregate quality on the mechanical properties of high strength concrete. *Construction and Building Materials, 17*(2), 97–103. https://doi.org/10.1016/S0950-0618(02)00097-1

Coppola, L., Buoso, A., Coffetti, D., Kara, P., & Lorenzi, S. (2016). Electric arc furnace granulated slag for sustainable concrete. *Construction and Building Materials, 123*, 115–119. https://doi.org/10.1016/j.conbuildmat.2016.06.142

Diotti, A., Cominoli, L., Pérez Galvin, A., Sorlini, S., & Plizzari, G. (2021). Sustainable recycling of electric arc furnace steel slag as aggregate in concrete: Effects on the environmental and technical performance. *Sustainability, 13*(2), 521. https://doi.org/10.3390/su13020521

Ernawan, E., Sjah, J., Handika, N., Astutiningsih, S., & Vincens, E. (2023). Mechanical properties of concrete containing ferronickel slag as fine aggregate substitute using digital image correlation analysis. *Buildings, 13*(6), 1463. https://doi.org/10.3390/buildings13061463

Fitriyanti, Ismawati, & Annisa, H. (2025). Evaluasi awal penggunaan slag nikel sebagai agregat halus pada beton self-compacting concrete (SCC). *Jurnal Teknik Sipil Macca, 10*(3), 278–287. https://doi.org/10.33096/c3g3f509

This work is licensed under a Creative Commons Attribution 4.0 International license

Irmawaty, R., Akbar, M., Tjaronge, C. M. W., Asad, M., & Ahmad, S. B. (2023). Compressive strength and corrosion behavior of steel bars embedded in concrete produced with ferronickel slag aggregate and fly ash: An experimental study. *Innovative Infrastructure Solutions, 8*. https://doi.org/10.1007/s41062-023-01162-1

Levene, H. (1960). Robust tests for equality of variances. In I. Olkin, S. G. Ghurye, W. Hoeffding, W. G. Madow, & H. B. Mann (Eds.), *Contributions to probability and statistics: Essays in honor of Harold Hotelling* (pp. 278–292). Stanford University Press.

Maslehuddin, M., Sharif, A. M., Shameem, M., Ibrahim, M., & Barry, M. S. (2003). Comparison of properties of steel slag and crushed limestone aggregate concretes. *Construction and Building Materials, 17*(2), 105–112. https://doi.org/10.1016/S0950-0618(02)00095-8

Mehta, P. K., & Monteiro, P. J. M. (2014). *Concrete: Microstructure, properties, and materials* (4th ed.). McGraw-Hill Education.

Nelfia, L. O., Haq, A. B. N., Nugroho, A., Rinanti, A., Yuwono, B. E., Syamsunur, D., Sunarno, Y., & Amiri, O. (2024). Comprehensive characteristics of high-performance concrete with nickel slag as fine and coarse aggregate. *International Journal of Technology, 15*(6), 1613–1631. https://doi.org/10.14716/ijtech.v15i6.7184

Neville, A. M. (2011). *Properties of concrete* (5th ed.). Pearson Education.

Nuruzzaman, M., Almeida, J., Amin, M. T. E., & Sarker, P. K. (2024). Performance of sustainable green concrete incorporating quarry dust and ferronickel slag as fine aggregate. *Materials, 17*(10), 2326. https://doi.org/10.3390/ma17102326

Nuruzzaman, M., Casimiro, J. O. C., & Sarker, P. K. (2020). Fresh and hardened properties of high-strength self-compacting concrete using by-product ferronickel slag fine aggregate. *Journal of Building Engineering, 32*, 101686. https://doi.org/10.1016/j.jobe.2020.101686

Nuruzzaman, M., Kuri, J. C., & Sarker, P. K. (2022). Strength, permeability, and microstructure of self-compacting concrete with the dual use of ferronickel slag as fine aggregate and supplementary binder. *Construction and Building Materials, 318*, 125927. https://doi.org/10.1016/j.conbuildmat.2021.125927

Rojas, N., Bustamante, M., Muñoz, P., Godoy, K., & Letelier, V. (2023). Study of properties and behavior of concrete containing EAF slag as coarse aggregate. *Developments in the Built Environment, 14*, 100137. https://doi.org/10.1016/j.dibe.2023.100137

Sandra, N., Caronge, M. A., Sunaryati, J., Kawaai, K., Nsama, W., Arbi, Y., & Arifin, A. S. R. (2025). Durability performances of ferronickel slag aggregate and seawater concrete. *Teknomekanik, 8*(1), 79–98. https://doi.org/10.24036/teknomekanik.v8i1.34572

Soundararajan, M., Jayaprakash, S., Maniarasan, S. K., & Gobinath, R. (2023). Predicting strength properties of high-performance concrete modified with natural aggregates and ferroslag under varied curing conditions. *Advances in Civil Engineering, 2023*, 9960412. https://doi.org/10.1155/2023/9960412

Suwindu, K. S., Parung, H., & Sandy, D. (2020). Karakteristik beton mutu tinggi dengan substitusi slag baja dan slag nikel sebagai agregat kasar. *Paulus Civil Engineering Journal*.

Tukey, J. W. (1949). Comparing individual means in the analysis of variance. *Biometrics, 5*(2), 99–114. https://doi.org/10.2307/3001913

Virtanen, P., Gommers, R., Oliphant, T. E., Haberland, M., Reddy, T., Cournapeau, D., Burovski, E., Peterson, P., Weckesser, W., Bright, J., van der Walt, S. J., Brett, M., Wilson, J., Millman, K. J., Mayorov, N., Nelson, A. R. J., Jones, E., Kern, R., Larson, E., … SciPy 1.0 Contributors. (2020). SciPy

This work is licensed under a Creative Commons Attribution 4.0 International license

1.0: Fundamental algorithms for scientific computing in Python. *Nature Methods, 17*(3), 261–272. https://doi.org/10.1038/s41592-019-0686-2